

Magnetic monopole relaxation effects probed by modulation calorimetry in small spin-ice samples

R. Edberg,¹ I. M. Fjellvåg,² L. Ørdu Sandberg,³ P. P. Deen,³ K. Lefmann,³ P. Henelius,^{4,5} and A. Rydh⁶

¹*Physics Department, KTH Royal Institute of Technology, Sweden*

²*Centre for Materials Science and Nanotechnology,*

Department of Chemistry, University of Oslo, Norway

³*Niels Bohr Institute, University of Copenhagen, Denmark*

⁴*Physics Department, KTH Royal Institute of Technology, Stockholm, Sweden*

⁵*Faculty of Science and Engineering, Åbo Akademi University, Åbo, Finland*

⁶*Department of Physics, Stockholm, Stockholm University, Sweden*

(Dated: February 8, 2022)

We use modulation calorimetry to study the heat capacity of small samples (30 ng – 10 μ g) of the classical spin-ice compounds $\text{Dy}_2\text{Ti}_2\text{O}_7$ and $\text{Ho}_2\text{Ti}_2\text{O}_7$ at low temperature (0.5 – 3 K). Using modulation frequencies of 0.1-200 Hz we find a strong frequency dependence in the measured heat capacity and are able to study thermal relaxation effects on the corresponding timescales. Performing dynamic Monte Carlo simulations we verify that the specific heat frequency response has its origin in the slow magnetic monopole dynamics indigenous to spin ice. We find a timescale of 20 ms per Monte Carlo step at 4 K in contrast to 2.5 ms mentioned in previous studies by other techniques¹. Our study establishes modulation calorimetry as a versatile experimental probe of dynamic processes in frustrated magnetic materials.

I. INTRODUCTION

In highly frustrated magnetic compounds the dynamic and static properties are frequently intertwined. The slow dynamics of excitations such as magnetic monopoles in the spin ice family of materials¹⁻³, the long timescales observed spin glasses^{4,5} or the motion of clusters in dilute magnets⁶ are examples where the experimental time window may influence the outcome of measurements of thermodynamic properties traditionally considered static, such as the specific heat. Deducing the material properties becomes challenging both experimentally and theoretically and this field has given rise to many longstanding questions such as the nature of the spin glass ground state^{4,5}.

Experimentally the dynamic properties are probed using for example out-of-phase magnetic susceptibility³, inelastic neutron scattering or muon spin resonance. In this study we probe the low-temperature dynamic properties of the classical spin ice compounds $\text{Dy}_2\text{Ti}_2\text{O}_7$ (DTO) and $\text{Ho}_2\text{Ti}_2\text{O}_7$ (HTO) using modulation calorimetry. This method offers several advantages; compared to inelastic neutron scattering the need for experimental facilities is modest and slower timescales can be probed as neutron scattering experiments typically probe timescales in the GHz to THz range. According to Griffiths's theorem⁷ the specific heat is independent of the sample shape in the absence of an applied magnetic field, and a potentially challenging demagnetization analysis⁸ is avoided, comparing to magnetic susceptibility. Furthermore, it is possible to perform the measurements on small samples of sub-mm size, which may be an advantage if it is difficult to synthesize large samples, or if the dynamical properties are strongly size dependent.

While AC susceptibility measurements in the 10^{-4} – 10^4 Hz frequency range has become a standard compli-

ment to static susceptibility investigations, the vast majority of specific heat measurements are performed as static relaxation measurements. The reason for this is partially due to instrumentation. The idea of modulation calorimetry dates back many years^{9,10}, but only recently has the method matured to yield absolute accuracy with the development of membrane-based calorimeters and resistive thin-film thermometry^{11,12}. This new level of accuracy now allows for the determination of the variable frequency and dynamic heat capacity, which we demonstrate in this study.

The timescales which can be accessed using modulation calorimetry, combined with the importance of specific heat as probe of central importance in magnetic systems makes this an ideal tool to investigate highly frustrated magnetic systems with slow dynamics. In this study we chose to focus on HTO and DTO since the low-temperature specific heat in these materials has been the subject of intense recent research^{13,14}. Theoretically a low-temperature ordering transition is predicted¹⁵ to occur at 0.2 K. Experimentally no signs of this transition had been detected¹⁶⁻¹⁹ until a relaxation specific heat study found clear signs of an impending upturn already at 0.5 K²⁰. The investigation considered very long relaxation processes of more than 100 hours per measurement point at the lowest temperature (0.34 K). Subsequent neutron investigations with in situ equilibration times of several weeks did not reproduce the findings²¹, and theoretical studies could not match the upturn²².

Modulation calorimetry offers the possibility to study small samples which can be kept in thermal equilibrium at high modulation frequencies. In analogy with magnetic susceptibility, the response from frequency modulation can be described with a complex heat capacity. The real and imaginary parts of the complex heat capacity have many of the same interpretations as other re-

sponse functions and are related by the Kramers-Kronig relations^{23,24}. In this work we measure the real part of the complex heat capacity, which is commonly termed the dynamic heat capacity. With smaller than previously measured samples and with use of this complimentary method we hope not only to extend the knowledge of low-temperature properties of spin ice but also to shed further light on complex heat capacity measurements in the context of magnetically frustrated compounds.

Our study finds a strong frequency dependence in the low-temperature (0.5-3 K) dynamic heat capacity of HTO and DTO in the frequency range of 0.1-200 Hz. Dynamic Monte Carlo studies of the general dipolar spin ice model²⁵ match the experimental results well and our main result is that the theory, where the main dynamic effects at low temperature arise from the motion of the magnetic monopole excitations, captures the temperature and frequency dependence of the dynamically measured heat capacity well. Therefore, we establish modulation calorimetry as a highly useful probe of slow magnetic processes, but we failed to find reproducible signs of an upturn in the specific heat at low (< 0.5 K) temperature.

II. EXPERIMENTAL METHOD AND RESULTS

Powders of both HTO and DTO are synthesized and single crystals of HTO are grown using the floating zone technique at the image furnace at Lund University, Sweden. The crystals are grown from the bottom up with a growth rate of 3 mm/hr. Visual inspection of the as-grown crystals revealed no color change along the growth direction as seen by others²⁶.

The crystals are polished to thin samples of varying aspect ratio: base approximately $100 \times 100 \mu\text{m}$ and thickness of about 100, 20 and 10 μm . To increase the thermal conductivity, the powder samples are either mixed in a 1:1 volumetric ratio with Apiezon N grease, or cold pressed in a 1:1 volumetric ratio with 99.99% pure, 3 μm Ag powder. The cold pressing method is generally used in the spin-ice literature, because it gives large sturdy samples and Ag has a negligible contribution to the heat capacity¹⁶. However, for small samples the surface tension of Apiezon N grease is enough to give the desired rigidity, and its contribution to the heat capacity is also negligible at low temperatures. We therefore believe that both methods work equally well for the intended purpose. The samples are mounted on a Si_3N_4 membrane calorimeter, which is connected to a thermal bath with a temperature of approximately 20 mK. The exact measurement procedure is described elsewhere¹¹, and in our study we measure a variety of powder and single crystal samples of different size and shape.

A. Thermal relaxation

In order to confirm that the materials are correctly synthesized and that the experimental setup is working with the desired precision for spin-ice compounds, we first perform thermal relaxation measurements. Powder of DTO is cold pressed with silver powder, and cut into a block of size approximately $800 \times 800 \times 500 \mu\text{m}$. The relaxation is performed by decreasing the applied power so that the temperature drops with about 50 steps per decade from 4 K to 0.1 K. The power $P_{\text{out}}(T)$ escaping through the thermal link is estimated from the equilibrium temperature at each step. We interpolate over these values, and find the heat capacity $C(T)$ by minimizing the residual between the solution of

$$\frac{dT}{dt} = \frac{P_{\text{in}}(t) - P_{\text{out}}(T(t))}{C(T)}, \quad (1)$$

and the experimental data. The heat capacity is assumed constant for each relaxation interval and $P_{\text{in}}(t)$ is the power applied via the heater.

The results are shown in Fig. 1. The measured heat capacity matches well with previous observations^{16,17}. The overall scale has been adjusted so that the intensity of the 1 K peak matches with literature, because the mass of the sample could not be determined with sufficient accuracy. The measured heat capacity is slightly lower at higher temperature compared with literature, and we believe that this is due to phonon contributions which can change with the mixing ratio and the sample holder used. For further investigations we plan to measure small masses directly using an electrostatic force balance²⁸ in order to eliminate a free parameter.

Hence we conclude that the setup has adequate resolution and is working correctly. It also confirms that the samples are correctly synthesized, since all samples are synthesized using the same method and equipment.

B. Modulation calorimetry

In Figure 2(a) we show heat capacity measurement obtained using modulation calorimetry for a DTO powder sample with an estimated size of 30 ng. Several measurements are performed to probe different modulation frequencies (f -range 1-5) ranging from 0.1 Hz to 200 Hz. The sample is mounted on a membrane and the exact measurement procedure is described elsewhere^{10,11}. The power $P(t)$ is modulated sinusoidally with frequency $f = (2\pi)^{-1}\omega$, resulting in a temperature oscillation $T_{\text{ac}}(t)$ of the sample¹¹

$$\begin{aligned} P(t) &= P_0(1 + \sin \omega t), \\ T_{\text{ac}}(t) &= T_{\text{ac},0} \sin(\omega t - \phi). \end{aligned} \quad (2)$$

Here, P_0 is a constant and by varying the input power and the modulation frequency, the amplitude of the temperature oscillations $T_{\text{ac},0}$ and its phase shift ϕ is set depending on the properties of the sample. By measuring

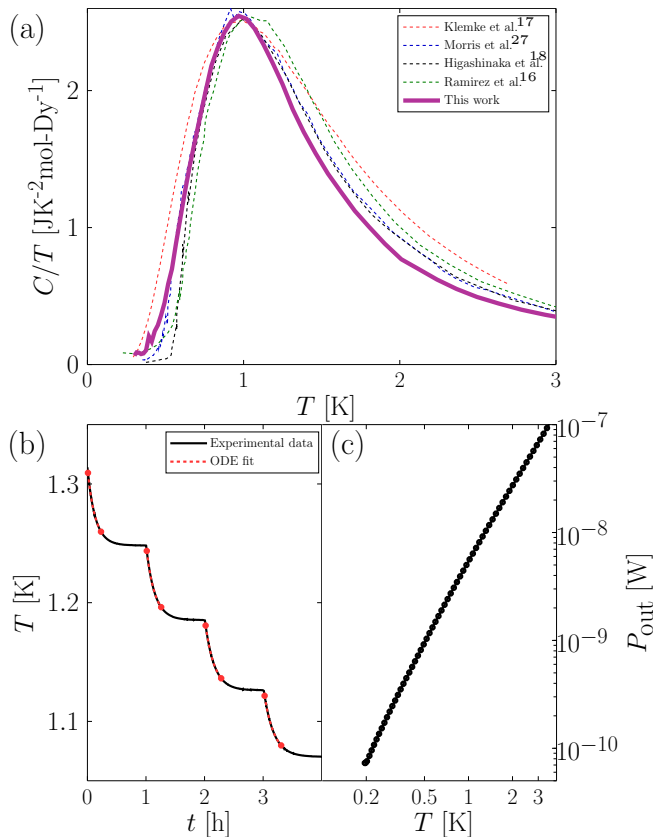


FIG. 1: Heat capacity and thermal relaxation properties of a DTO powder sample cold pressed with silver powder. (a) Our heat capacity values compared with four data sets from literature. (b) Thermal relaxation to which the solution of Eq. (1), (ODE fit), is fitted to determine $C(T)$ shown in red. (c) Experimentally measured P_{out} as function of temperature, used in Eq. (1)

these quantities, the heat capacity can be computed according to¹⁰

$$T_{\text{ac},0} = \frac{P_0}{\sqrt{(\omega C)^2 + \kappa^2}}, \quad (3)$$

$$\tan \phi = \frac{\omega C}{\kappa}.$$

For this measurement technique it is advantageous¹¹ to adjust the frequency such that the phase shift between power and temperature, ϕ , is kept constant. The frequency used therefore varies with temperature as is presented in Fig. 2(b), where each curve, f -range 1-5, corresponds to a preset ϕ . The temperature offset due to the AC heater power is always a constant fraction of T as well.

Figure 2 establishes a clear frequency dependence in the measured dynamic heat capacity. For low modulation frequencies the dynamic heat capacity approaches

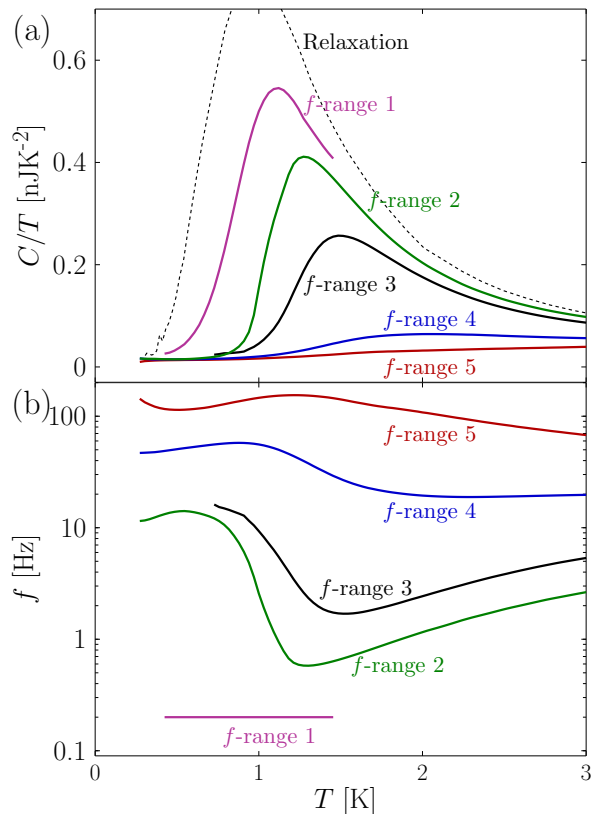


FIG. 2: (a) Experimentally measured heat capacity for 30 ng powder sample of DTO mixed with Apiezon N grease. The different curves show the heat capacity at different modulation frequencies in the 0.1 Hz to 200 Hz range. The dashed line shows the result from the relaxation measurement of Fig. 1 corresponding to the zero frequency limit. It has been scaled to fit the modulation measurements at 4 K. (b) Modulation frequency as function of temperature.

the conventionally measured static value, with a characteristic spin-ice peak centered at 1 K. When the frequency is increased, this feature is suppressed and the maximum is shifted to higher temperatures. In the limit of high frequency, the heat capacity is reminiscent of a pure phononic contribution.

Figure 3 shows the equivalent results for an approximately cubic HTO single crystal with side length $100 \mu\text{m}$ and a mass of approximately $7 \mu\text{g}$. For this sample, we fix the modulation frequency and keep it constant during the different measurements. The qualitative features are the same: when the frequency is increased, the peak in the heat capacity decreases. For HTO the interpretation is more complicated due to a dominating nuclear contribution to the specific heat appearing below 1 K²⁹. We find that the nuclear contribution is also strongly suppressed at higher frequency. In order to quantitatively reproduce the previous results²⁹ we would need lower probing frequencies. Experimentally this would require a bigger sample, since low-frequency measurements on a

small sample are prone to phase errors.

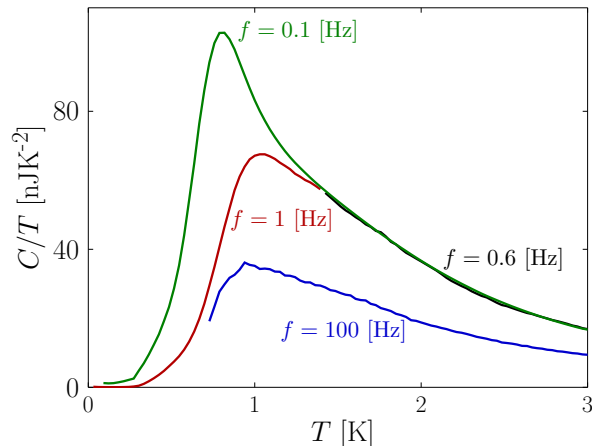


FIG. 3: Heat capacity measurement of a single crystal of HTO using modulation calorimetry. For the lowest frequencies the nuclear contribution starts to develop below $T = 1$ K. As in the case of DTO the measured heat capacity decreases when the frequency is increased.

III. THEORETICAL ANALYSIS

A. Thermal conductivity

The frequency dependence in the heat capacity measurement signals that the system is out of equilibrium. The observed non-equilibrium contributions to the heat capacity can be due to several causes. A natural starting point is to investigate the heat transport in spin ice, which is mediated by spin and phonon interactions. The steady state thermal conductivity of DTO has been studied previously^{17,30} and it was concluded that the largest contribution to the thermal conductivity in the 1 K range is due to phonons. By application of magnetic fields it was also found that magnetic monopoles transport heat as a smaller secondary effect.

Based on the available heat conductivity data from one of the studies³⁰, we estimate the typical response to modulation calorimetry for our sample. To do this, we simulate the heat equation for a sphere with sinusoidally varying surface temperature,

$$C_V(T(r, t)) \frac{\partial T(r, t)}{\partial t} = r^{-2} \frac{\partial}{\partial r} \left(r^2 \kappa(T(r, t)) \frac{\partial T(r, t)}{\partial r} \right), \quad (4)$$

where the thermal conductivity κ and the specific heat $C_V \equiv C/V$ are temperature dependent with values according to experimental observations³⁰. The sphere resembles the average shape of a powder grain, but the

results may also be used to make order of magnitude estimates for single crystal samples. The surrounding Ag or Apiezon N grease both have high thermal conductivity in comparison to DTO and we do not need to consider their contribution for this estimate.

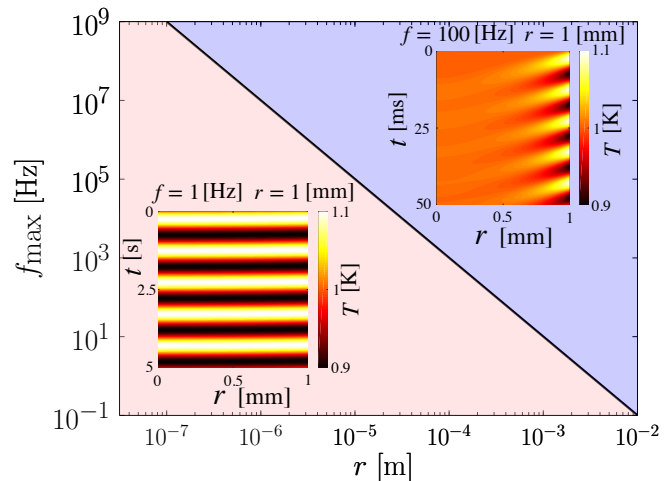


FIG. 4: Theoretical upper frequency f_{\max} that can be used to probe a spherical DTO sample of radius r . The upper frequency is an estimate above which the temperature modulations in the core have an amplitude less than 10% of the surface amplitude. Pink area: core and surface are at equal temperature resulting in reliable results from modulation calorimetry. Blue area: surface modulations are too fast and the core does not have time to equilibrate, resulting in a smaller measured heat capacity than the actual value. The insets show the typical solution to the heat equation, Eq. (4), in the respective regimes for a 1 mm radius sphere of DTO.

If the frequency is high, and the temperature gradients consequently are large, the temperature oscillations at the center of the sample will have smaller amplitude than those at the surface. This will result in a lower measured heat capacity, since the whole sample does not participate in the heat exchange.

The heat equation allows us to determine the extent of this effect and we can determine an upper limit for the frequency that can be used to probe a sample while maintaining low thermal gradients. Figure 4 shows the maximum allowed frequency f_{\max} as a function of sample size for a spherical DTO sample of radius r . The insets show the typical solutions to the heat equation in the two different regimes. Above the maximum frequency, f_{\max} , the temperature is not homogeneous in the sample, resulting in a lower value of the measured heat capacity. For a sample with radius 1 mm, the thermal conductivity is sufficient for frequencies up to 1 Hz (left inset in Fig 4). However, with a surface modulation frequency of 100 Hz the temperature oscillations affect only the surface, and the interior of the sample will not give any contribution to the measured heat capacity (right inset in Fig. 4).

If we probe below the critical modulation frequency, the temperature gradients are small and we will observe the full heat capacity of the sample. This is the case for the experiments performed in this study, since the largest sample is about 100 μm large and the maximum frequency used is less than 200 Hz. Hence, the observed experimental behavior is not due to poor thermal conductivity. Instead, it is likely to originate in the slow low-temperature magnetic dynamics inherent to spin ice. With sufficiently slow dynamics a delay in the spin system temperature can develop with respect to the phonon system which can explain the observed features in the heat capacity^{31,32}.

B. Monte Carlo

Inspired by the results in the previous section, we assume that the sample has a uniform temperature distribution and that the heat conduction through phonons is good. To evaluate whether the slow dynamics of the monopole excitations can give rise to the observed frequency dependence in the specific heat we perform dynamic Monte Carlo (MC) simulations for the general dipolar spin ice Hamiltonian^{25,33},

$$\begin{aligned} \mathcal{H} = & J_1 \sum_{\langle i,j \rangle_1} \mathbf{S}_i \cdot \mathbf{S}_j + J_2 \sum_{\langle i,j \rangle_2} \mathbf{S}_i \cdot \mathbf{S}_j \\ & + J_{3a} \sum_{\langle i,j \rangle_{3a}} \mathbf{S}_i \cdot \mathbf{S}_j + J_{3b} \sum_{\langle i,j \rangle_{3b}} \mathbf{S}_i \cdot \mathbf{S}_j \\ & + D a^3 \sum_{i < j} \left(\frac{\mathbf{S}_i \cdot \mathbf{S}_j}{|\mathbf{r}_{ij}|^3} - 3 \frac{(\mathbf{S}_i \cdot \mathbf{r}_{ij})(\mathbf{S}_j \cdot \mathbf{r}_{ij})}{|\mathbf{r}_{ij}|^5} \right), \end{aligned} \quad (5)$$

where \mathbf{S}_i are unit Ising spins on the pyrochlore lattice, with Ising axis along the local $\langle 111 \rangle$ directions. The nearest-neighbor distance is denoted by a and the parameters J_1 , J_2 and $J_{3a,b}$ are the first- second- and third-neighbor exchange interactions respectively. The reason for having two different types of third-neighbor interactions is that third-neighbor pairs can have two different local environments. Analogously $\langle \dots \rangle_{i(a,b)}$ denotes summation over the i :th nearest-neighbor pairs. We use the g^+ -DSM parameters³³ $J_1 = 3.41$ K, $J_2 = -0.14$ K, $J_{3a} = 0.030$ K and $J_{3b} = 0.031$ K. The simulated supercell is cubic and built from L^3 standard unit cells¹⁹ with $L \in [1, \dots, 8]$.

The simulation is performed in the following way: the system is equilibrated at a given temperature, T_0 , using the Metropolis Hastings heat-bath algorithm¹⁹. The process of modulation calorimetry is then emulated by changing the temperature in the Boltzmann weight according to

$$T = T_0 + T_{AC} \sin(2\pi f g(T) t_{MC}), \quad (6)$$

where $g(T)$ is a conversion factor from MC time, t_{MC} , to real time, f is the modulation frequency, T_0 is the

measured temperature and T_{AC} is the amplitude of the modulation. A small value of T_{AC} gives the most accurate results at the cost of slow MC convergence. We find that having T_{AC} set to 1% or 10% of the measured temperature gives the same simulation result and set it to 10% for quicker convergence. Single spin-flip updates are performed at random sites in the simulation-cell with the oscillating Boltzmann weight. Every update emulates a direct spin-phonon interaction³¹, and the Boltzmann weight reflects the interaction with a phonon-bath with oscillating temperature. The frequency dependence is emulated by letting the number of update attempts in a modulation period be inversely proportional to the frequency. For high frequencies, there are few updates per period. For low frequencies, there are many updates per period. This reflects that the number of spin-phonon interactions per time is constant. The temperature dependence of $g(T)$ has been introduced because there are fewer phonon modes available at low temperatures. A random collision (Monte Carlo update) therefore takes longer time to occur at low temperatures. We assume that during one second the number of spin-phonon interactions is $n(T)$ and that this follows an Arrhenius distribution,

$$n(T) = n^0 e^{-\theta/T}. \quad (7)$$

The constants n^0 and θ are free parameters which determine the relationship between MC time and real time and need to be fitted to experimental measurements. With this assumption, the conversion factor between MC time and real time can be expressed as:

$$g(T) \equiv \frac{1}{n(T)} = \frac{e^{\theta/T}}{n^0}. \quad (8)$$

since there are $n(T)$ MC steps per second.

The heat capacity is calculated by fitting a linear interpolation to a E vs T diagram. We also add the theoretical phonon contribution according to the Debye model^{17,34}:

$$C_{ph}(T) = 9n_{Dy} k_B N_A \left(\frac{T}{\theta_D} \right)^3 \cdot \int_0^{\theta_D/T} \frac{x^4 e^x}{(e^x - 1)^2} dx, \quad (9)$$

where $n_{Dy} = 11$ is the number of atoms per molecule $\text{Dy}_2\text{Ti}_2\text{O}_7$ and we use the Debye temperature $\theta_D = 283$ K¹⁷. We compare the calculated heat capacity with the experiment and choose n^0 and θ to get the best possible fit. The size of the sample is also fitted, since it could not be determined with the needed accuracy. Hence we fit a total of three parameters to the experimental data, but with a more controlled experiment we believe that only two free parameters are needed.

IV. RESULTS AND DISCUSSION

From the MC simulations in the previous section, we found that the values $n^0 = 80$ and $\theta = 2$ K gave the

best fit, Fig. 5. From the figure it is clear that the main features of the experiment are in excellent agreement with the simulation. This suggests that the frequency dependence in the experimental data is due to magnetic monopole relaxation effects and hence gives a new way of investigating the behavior of monopoles in spin ice. For the highest frequencies, f -range 4-5, there is some discrepancy between the experiment and the MC simulation. In particular there is a constant contribution to the experimental heat capacity which can not be fully explained by the model. In the figure we also show explicitly the contribution of the Debye model, Eq. (9), which has been added to all MC curves. For f -range 5 the theoretical heat capacity is almost only due to this contribution. That is: the simulation is too fast to capture any magnetic contribution.

Compared to other techniques, the value $\theta = 2$ K is in the same order of magnitude as the previously reported value of 4.5 K³, found by susceptibility measurements. Furthermore, inserting n^0 and θ in $g(T)$ we find that it takes about 100 ms for one MC step at 1 K. By extrapolation to $T = 4$ K we obtain 20 ms per MC step in contrast to 2.5 ms mentioned in previous studies¹. The discrepancy is worth noting and can have several causes. The previous study uses a different technique for studying the relaxation phenomena, which can have resulted in a timescale characteristic for that experiment. Another possible cause of the discrepancy is an oversimplification in treating MC time like real time. Nevertheless, the excellent fit with experimental data indicates that the approximation can still give a good description of the underlying physical properties.

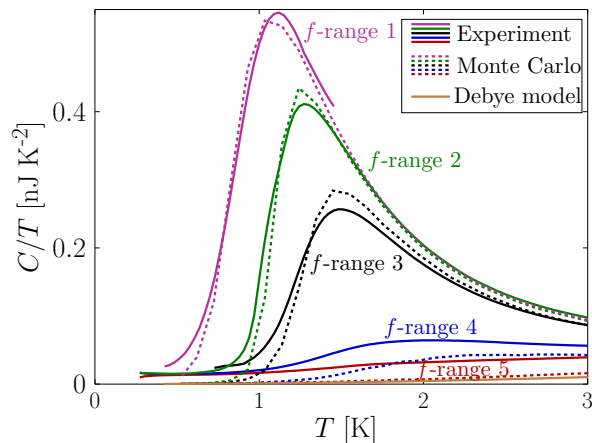


FIG. 5: Theoretical MC simulation for $n^0 = 80$ and $\theta = 2$ K for $L = 3$ (dashed) together with experimental data (solid) for a DTO powder sample. The frequencies used for the different curves are the same as those shown in Fig. 2(b) (f -range 1-5). The contribution from the Debye model has been included in the theoretical curves, and is also plotted independently.

V. CONCLUSION

Many recent experimental and theoretical studies have aimed to recover of the "lost" Pauling entropy, and to find signs of the associated peak in the specific heat originating in a low-temperature phase transition at about 0.1 K. Using a variety of sample sizes from tiny single crystals and small pressed powder samples to much larger single crystals and powder samples we carefully looked for signs of an ordering transition in the 0.1-0.2 K temperature range, but failed to see any signs in the frequency range accessible with our experimental setup. Whether this is due to a timescale that is too long, or some other physical effects, possibly of quantum mechanical origin, that preempt such a transition could not be determined in this study.

On the other hand, we have found that modulation calorimetry in the frequency range 0.1-200 Hz is a very suitable experimental probe for studying thermal relaxation effects in the classical spin ice compounds DTO and HTO. Within this frequency range the spin ice peak centered around 1 K changes from almost fully developed (0.1 Hz) to a pure phonon contribution (200 Hz). We expect that modulation calorimetry will become a standard tool for investigating low-temperature slow dynamics in a wide range of highly frustrated magnetic compounds.

ACKNOWLEDGMENTS

The simulations were performed on resources provided by the Swedish National Infrastructure for Computing (SNIC) at the Center for High Performance Computing (PDC) at the Royal Institute of Technology (KTH). The project was supported by Nordforsk through the program NNSP (Project No. 82248) and by the Danish Agency for Research and Innovation through DANSCATT.

-
- ¹ L. D. C. Jaubert and P. C. W. Holdsworth, *J. Phys.: Condens. Matter* **23**, 164222 (2011).
- ² L. D. C. Jaubert and P. C. W. Holdsworth, *Nature Physics* **5**, 258 (2009).
- ³ H. M. Revell, L. R. Yaraskavitch, J. D. Mason, K. A. Ross, H. M. L. Noad, H. A. Dabkowska, B. D. Gaulin, P. Henelius, and J. B. Kycia, *Nature Physics* **9**, 34 (2013).
- ⁴ K. Binder and A. P. Young, *Rev. Mod. Phys.* **58**, 801 (1986).
- ⁵ J. A. Mydosh, *Rep. Prog. Phys.* **78**, 052501 (2015).
- ⁶ A. Biltmo and P. Henelius, *Nature Communications* **3**, 857 (2012).
- ⁷ R. Griffiths, *Phys. Rev.* **176**, 655 (1968).
- ⁸ M. Twengström, L. Bovo, M. J. P. Gingras, S. T. Bramwell, and P. Henelius, *Phys. Rev. Materials* **1**, 044406 (2017).
- ⁹ P. F. Sullivan and G. Seidel, *Physical Review* **173**, 679 (1968).
- ¹⁰ E. Gmelin, *Thermochimica Acta* **304-305**, 1 (1997), temperature Modulated Calorimetry.
- ¹¹ S. Tagliati and A. Rydh, *Thermochimica Acta* **522**, 66 (2011), special Issue: Interplay between Nucleation, Crystallization, and the Glass Transition.
- ¹² S. Tagliati, V. M. Krasnov, and A. Rydh, *Review of Scientific Instruments* **83**, 055107 (2012).
- ¹³ C. Castelnovo, R. Moessner, and S. Sondhi, *Annual Review of Condensed Matter Physics* **3**, 35 (2012), <https://doi.org/10.1146/annurev-conmatphys-020911-125058>.
- ¹⁴ S. T. Bramwell and M. J. Harris, *Journal of Physics: Condensed Matter* **32**, 374010 (2020).
- ¹⁵ R. G. Melko, B. C. den Hertog, and M. J. P. Gingras, *Phys. Rev. Lett.* **87**, 067203 (2001).
- ¹⁶ A. P. Ramirez, A. Hayashi, R. J. Cava, R. Siddharthan, and B. S. Shastry, *Nature* **399**, 333 (1999).
- ¹⁷ B. Klemke, M. Meissner, P. Strehlow, K. Kiefer, s. Grigera, and A. Tennant, *Journal of Low Temperature Physics* **163**, 345 (2011).
- ¹⁸ H. Y. D. Higashinaka R., Fukazawa and M. Y., *J. Phys. Chem. Solids* **63**, 1043–1046 (2002).
- ¹⁹ R. G. Melko and M. J. P. Gingras, *Journal of Physics: Condensed Matter* **16**, R1277 (2004).
- ²⁰ D. Pomaranski, L. R. Yaraskavitch, S. Meng, K. A. Ross, H. M. L. Noad, H. A. Dabkowska, B. D. Gaulin, and J. B. Kycia, *Nature Physics* **9**, 353 (2013).
- ²¹ S. R. Giblin, M. Twengström, L. Bovo, M. Ruminy, M. Bartkowiak, P. Manuel, J. C. Andresen, D. Prabhakaran, G. Balakrishnan, E. Pomjakushina, C. Paulsen, E. Lhotel, L. Keller, M. Frontzek, S. C. Capelli, O. Zaharko, P. A. McClarty, S. T. Bramwell, P. Henelius, and T. Fennell, *Phys. Rev. Lett.* **121**, 067202 (2018).
- ²² P. Henelius, T. Lin, M. Enjalran, Z. Hao, J. G. Rau, J. Al-tosaar, F. Flicker, T. Yavors’kii, and M. J. P. Gingras, *Phys. Rev. B* **93**, 024402 (2016).
- ²³ H. Baur and B. Wunderlich, *Journal of Thermal Analysis and Calorimetry* **54**, 437 (1998).
- ²⁴ M. J. de Oliveira, *J. Stat. Mech* (2019).
- ²⁵ T. Yavors’kii, T. Fennell, M. J. P. Gingras, and S. T. Bramwell, *Phys. Rev. Lett.* **101**, 037204 (2008).
- ²⁶ A. Ghasemi, A. Scheie, J. Kindervater, and S. Koohpayeh, *Journal of Crystal Growth* **500**, 38 (2018).
- ²⁷ D. J. P. e. a. Morris, *Science* **326**, 411–414 (2009).
- ²⁸ G. A. Shaw, J. Stirling, J. A. Kramar, A. Moses, P. Abbott, R. Steiner, A. Koffman, J. R. Pratt, and Z. J. Kubarych, *Metrologia* **53**, A86 (2016).
- ²⁹ S. T. Bramwell, M. J. Harris, B. C. den Hertog, M. J. P. Gingras, J. S. Gardner, D. F. McMorro, A. R. Wildes, A. L. Cornelius, J. D. M. Champion, R. G. Melko, and T. Fennell, *Phys. Rev. Lett.* **87**, 047205 (2001).
- ³⁰ G. Kolland, O. Breunig, M. Valldor, M. Hiertz, J. Frielingsdorf, and T. Lorenz, *Phys. Rev. B* **86**, 060402 (2012).
- ³¹ K. J. Standley and R. A. Vaughan, (1969), <https://www.springer.com/gp/book/9781489962515>.
- ³² A. S. Oja and O. V. Lounasmaa, *Rev. Mod. Phys.* **69**, 1 (1997).
- ³³ L. Bovo, M. Twengström, O. A. Petrenko, T. Fennell, M. J. P. Gingras, S. T. Bramwell, and P. Henelius, *Nature Communications* **9**, 1999 (2018).
- ³⁴ S. J. Blundell, *Concepts in Thermal Physics* (Oxford University Press, 2009).